Transformations of graphitelike B-C phases under dynamic laser-driven pressure loading

T. de Rességuier*
Laboratoire de Combustion et de Détonique (UPR 9028), ENSMA, 1 Ave. Clément Ader, F-86961 Futuroscope, France

V. L. Solozhenko, J. P. Petitet, and O. O. Kurakevych
Laboratoire des Propriétés Mécaniques et Thermodynamiques des Matériaux (UPR 9001), Université Paris Nord, F-93430 Villetaneuse, France

E. Lescoute
Laboratoire de Combustion et de Détonique (UPR 9028), ENSMA, 1 Ave. Clément Ader, F-86961 Futuroscope, France
(Received 1 February 2009; published 3 April 2009)

The response of graphitelike boron-carbon phases to shock wave loading has been investigated using short laser-driven pressure pulses. The main motivation, related to wide technological applications, was to study the possibility to synthesize via dynamic compression the B-doped diamond produced recently under high static pressures and temperatures. Over the explored range of shock pressure, no formation of such diamondlike phase has been observed. Instead, Raman and x-ray diffraction studies of the recovered samples have shown presence of mixtures of disordered graphite and boron carbide. Quantitative analysis of shock and release wave propagation in the multilayered targets has been performed, combining time-resolved measurements and simulations. It was found that despite the high amplitudes of the laser shocks, up to about 70 GPa, the pressure and temperature transmitted into the B-C specimens probably outlaid the p-T conditions required for the phase transition into diamondlike structures.

DOI: 10.1103/PhysRevB.79.144105 PACS number(s): 62.50.Ef, 81.30.−t, 83.60.Uv

I. INTRODUCTION

The synthesis of superhard materials more thermally and chemically stable than pure diamond is an issue of key interest for many engineering applications, from cutting or polishing of hard metals to microelectronics.[1,2] Graphitelike B-C phases have been studied under static compression, and a bulk composite material with hardness comparable to that of single-crystal diamond has been synthesized from graphitelike BC_3 under static compression to 20 GPa at about 2300 K.[3] The material consists of intergrown boron carbide B_4C and boron-doped (~1.8 at. % B) diamond. Very recently, the superhard single-phase c-BC_5 has been synthesized at high pressures and high temperatures from turbostratic BC_5 precursor.[4] Such solid-state phase transformations can also be induced by dynamic pressure produced by shock loading.[5–9] On one hand, shock compression techniques allow treating larger amounts of precursor than common large-volume multianvil presses. On the other hand, the efficiency may be limited by the kinetics of the transformations. For example, the polymorphic transitions occurring in quartz under short pulsed pressure loads induced by laser irradiation have been shown to differ substantially from the equilibrium phase diagram of silica.[10,11] Kinetic inhibitions may prevent diffusive transformations on the short time scales involved in dynamic compression experiments, whereas metastable structures may be quenched outside their stability range upon ultrafast pressure release.[12]

Here, we report on the results of investigation of graphitelike B-C phases under laser-driven shock compression. The main objective was to study the possibility to synthesize diamondlike B-C phases under dynamic loading and to shed some light on the early stages of the transformation.

II. EXPERIMENTAL

The experiments have been performed at the "nano2000" laser facility, LULI (Laboratoire pour l'Utilisation des Lasers Intenses, Ecole Polytechnique, Palaiseau, France) and at the "Alisé" laser facility, CESTA (Centre d'Etudes Scientifiques et Techniques d'Aquitaine, CEA, Le Barp, France). The B-C specimens of different stoichiometries (BC, BC_3, and B_2C_3) have been synthesized by thermal chemical-vapor deposition[13] in the form of 30–50 μm-thick chips with lateral dimensions from 2 to 3 mm. The chips were inserted between a thin aluminum covering foil and a thicker metallic backing plate, in a 40–70 μm-thick epoxy glue layer (Fig. 1). In all experiments conducted in the LULI, the backing plates were 2-mm-thick Al foils. In the lower intensity shots performed in the CESTA, they were 1–2 mm-thick Au foils.

A high-power pulsed Nd-glass laser beam of 1.06 μm wavelength and pulse duration of 4 or 7 ns was focused onto the Al foil. The diameter of the irradiated spot varied from 2 to 4.5 mm. The setup was placed in a vacuum chamber to avoid laser breakdown in air before reaching the target sur-

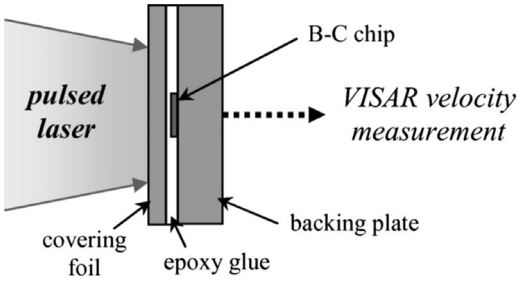

FIG. 1. Schematic view of the cross section of the experimental setup.

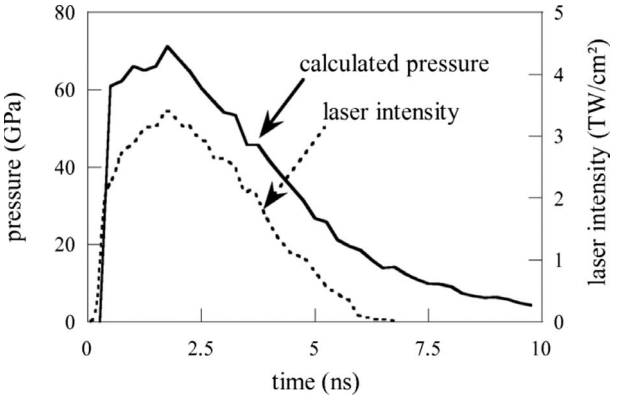

FIG. 2. Typical measured profile of laser intensity (dotted line, right scale) and corresponding pressure pulse calculated near the irradiated surface (solid line, left scale), for shot B_2C_3 No. 1.

face. The laser irradiation caused the vaporization of a thin layer of Al, transformed into a plasma cloud, which expansion toward the laser source drives by reaction a compressive pulse into the target assembly. The amplitude of this pressure load and its temporal shape were inferred from one-dimensional computations of laser-matter interaction, using the measured profile of laser intensity as input for the Lagrangian code FILM developed at the LULI. The resulting pulse consists of a sharp compression to a peak pressure maintained during a few ns, followed by slower unloading down to ambient pressure (Fig. 2). A velocity interferometer system for any reflector (VISAR) (Refs. 14 and 15) was used to measure the velocity of the free surface of the backing plate, opposite to the loaded surface. The values of the main experimental parameters are listed in Table I, as well as pressure and temperature values that are discussed later. After each shot, the recovered target was observed with optical (Carl Zeiss) and scanning electron (JSM-6400, JEOL) microscopes. When significant amount of shocked B-C material was recovered, it was investigated using Raman spectroscopy [LabRAM micro-Raman spectrometer, Jobin-Yvon, equipped with a large 1024 pixel charge-coupled device (CCD) chip that allows resolution from 0.3 to 1 cm^{-1} in the wave-number range between 200 and 4000 cm^{-1}] and powder x-ray diffraction (G3000 TEXT diffractometer, Inel, employing Cu $K\alpha_1$ radiation in Bragg-Brentano geometry).

III. VELOCITY MEASUREMENTS AND POSTSHOCK OBSERVATIONS

During propagation from the loaded surface, the compression front gets steeper and the release wave spreads, so the pressure profile becomes essentially triangular, and the peak pressure decays. Time-resolved measurements of the free-surface velocity have been combined to computer simulations to evaluate the pressure history throughout the target, taking into account the evolution of the pressure pulse during its propagation. For clarity, the discussion here is limited to the LULI experiments, where both the covering foils and the backing plates are made of Al. For each shot, a one-dimensional simulation of wave propagation has been performed with our Lagrangian hydrocode SHYLAC, where the loading pressure pulse inferred from the computation of laser-matter interaction (see Sec. II and Table I) is applied on the surface of a three-layered target consisting of two Al foils separated by epoxy glue. Thus, the presence of the thin B-C chip inserted in the glue is disregarded in the calculation, since the mechanical properties of that component are essentially unknown, and because this thin layer is expected to reach rapidly the equilibrium pressure induced in the surrounding material. For comparison, two additional laser shots have been performed on single-layer 2-mm-thick Al specimens.

Typical free-surface velocity records are shown in Fig. 3, (a) for the shots on single Al specimens and (b) for two shots on multilayered targets containing B_2C_3 chips. In all cases, the shock breakout at the free surface produces a steep ve-

TABLE I. Main experimental parameters, peak loading pressures calculated for the irradiated surface (irr. surf.) and for the sample location (sample loc.) that is in the glue layer between the covering foil and the backing plate and estimated peak temperature in the glue layer.

Shot ref.	Target materials and thicknesses (μm)	Laser facility	Laser energy (J)	Pulse duration (ns)	Spot diameter (mm)	Loading pressure (GPa)		Estimated temperature (K)
						Irr. surf.	Sample loc.	
B_2C_3 No. 1	Al(200)-B_2C_3-Al(2000)	LULI	1318	4	3.5	71	21.5	2200
B_2C_3 No. 2	Al(200)-B_2C_3-Al(2000)	LULI	1230	4	4	58	17	1640
BC_3 No. 1	Al(200)-BC_3-Al(2000)	LULI	1259	4	4.5	48	17	1640
BC_3 No. 2	Al(200)-BC_3-Al(2000)	LULI	1252	4	4	60	22	2290
Al No. 9	Al(1995)	LULI	1100	4	3.9	59		
Al No. 10	Al(2000)	LULI	995	4	3.9	55		
BC_3 No. 5	Al(40)-Au(30)-BC_3-Au(970)	CESTA	199	7	2	26	14	1300
B_2C_3 No. 6	Al(100)-Au(30)-B_2C_3-Au(970)	CESTA	200	7	2.1	21	10	900
BC No. 3	Al(40)-Au(30)-BC-Au(970)	CESTA	97	7	2	14	6	580
BC No. 2	Al(100)-Au(30)-BC-Au(2000)	CESTA	158	7	2.1	17	7.5	690

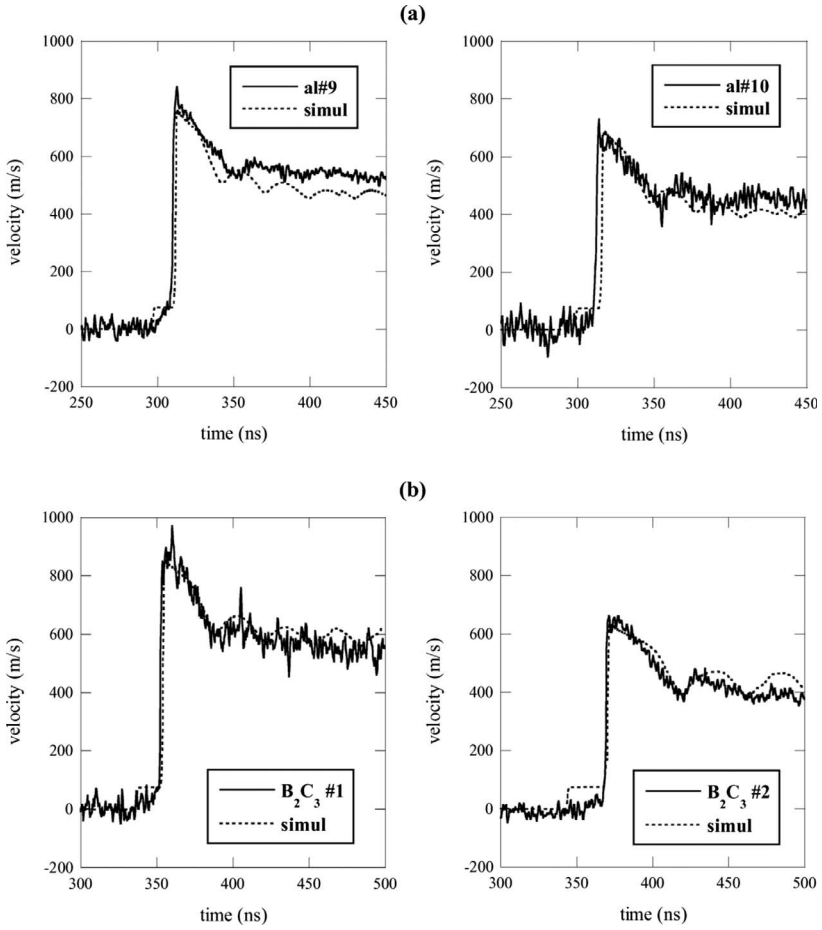

FIG. 3. (a) Free-surface velocity profiles measured at the back of single aluminum specimens and (b) multilayered targets (see Fig. 1) containing B_2C_3 chips, subjected to laser driven shocks in the LULI facility (see Table I). The profiles in dotted lines result from computations in which the presence of the B-C layer is ignored.

locity jump, followed by a gradual deceleration associated with the incident unloading wave. The interaction of this unloading wave with the release front reflected from the free surface induces tensile stresses of increasing magnitude, until spall fracture occurs at some distance beneath the free surface.[16] The subsequent relaxation of local tension produces a compressive disturbance, which propagates from the spall plane to the free surface, where its emergence is manifested as a characteristic reacceleration called the spall pulse. For each shot, the computed velocity profile is plotted in dotted lines. The elastic-plastic behavior of Al is modeled with a simple Von Mises constitutive law, which leads to steep elastic precursors, much sharper than in the records, ahead of the main acceleration fronts. The spall process is described with a phenomenological model from the literature,[17] which has been shown appropriate in laser shock-loading conditions.[18,19] The threshold tensile stress for damage initiation in Al has been increased from the original value of 1.5 GPa proposed in Ref. 19 to a slightly higher value of 1.8 GPa, which allows a better fit of the measured spall pulses.

The overall consistency between measured and computed profiles indicates to some extent the ability of the simulations to predict the pressure spatial and temporal distributions throughout the targets. In particular, the pressure history induced at the sample position (i.e., in the glue layer) can be calculated. Due to the attenuation through the covering foil and to the impedance mismatch between Al and epoxy, the peak pressure in the glue is considerably lower than the shock pressure applied onto the irradiated surface. In some shots, the variation of this peak pressure with depth inside the glue layer can reach a few GPa. Since the actual distance from the Al-epoxy interface to the B-C chip is essentially unknown, the pressure values given in Table I have been averaged over the thickness of the glue layer. Because the acoustic impedance (product of density and sound speed) of B-C is likely to be greater than that of epoxy, a transit state of higher pressure is probably induced in the B-C specimen before reaching the equilibrium pressure in the surrounding material, but this effect is hard to quantify without accurate determination of the thickness and shock properties of each layer. Still, the similarity between the velocity profiles measured at the free surfaces of single Al samples and multilayered targets (see Fig. 3) seems to confirm that the presence of B-C does not have a major effect on wave propagation. Since the covering foil prevents any heating of the glue layer via conduction from the laser generated plasma, the temperature history in the B-C specimen is governed by shock compression. Estimates of the peak temperatures induced in the glue have been inferred from shock wave data for epoxy.[20] They are reported in Table I. Like the pressure, the actual temperature reached in the B-C specimen itself is hard to evaluate without more accurate characterization of its mechanical and thermal properties.

Figure 4 shows (a) a schematic view of the targets recovered after the shot BC_3 No. 1, as well as (b) micrographs of

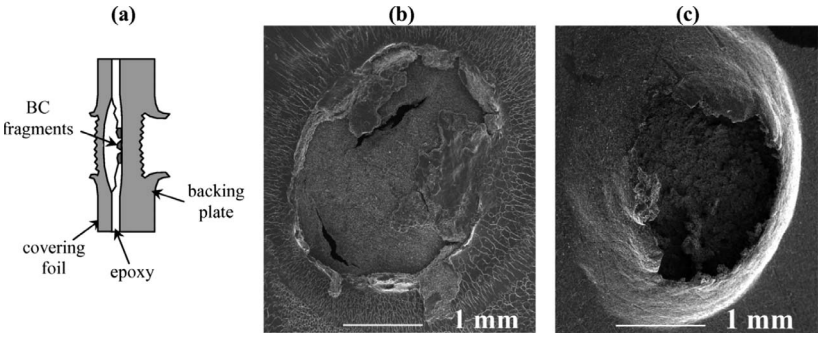

FIG. 4. (a) Schematic cross section of the target recovered after a 48 GPa laser shock (shot BC_3 No. 1) applied onto the left surface and scanning electron micrographs of the (b) covering Al foil and (c) backing Al plate. Both pictures are typical of spall craters caused by the interaction of release waves in the target assembly.

the front surface of the covering foil and (c) rear free surface of the backing plate. The craters shown on both surfaces are typical of the ejection of spalled layers. Such spallation process was expected beneath the rear free surface of the backing plate, upon reflection of the transmitted pressure pulse,[16] and it could be inferred from the spall pulse in the free-surface velocity record. On the other hand, spall fracture in the covering foil was unexpected. It results from the interaction of the incident unloading wave with a reflected release wave propagating back from the Al-epoxy interface, due to the impedance mismatch between those two layers. This reflected wave also explains the residual curvature of the foil toward the laser source. Those effects are reproduced by the computations, as shown in Fig. 5. Thin white rids developing radially outside the central crater [Fig. 4(b)] are typical of the expansion of a laser-generated plasma. The postshock situation after all shots of moderate intensity is essentially the same. In those experiments, most of the B-C samples could be recovered between the covering and backing Al components [Fig. 4(a)]. Figure 6 shows the postshock situation observed for laser shots of higher intensity, where the peak loading pressure is about 60–70 GPa (BC_3 No. 2 and B_2C_3 No. 1). The covering foil is heavily deformed toward the laser source, with a large circular hole matching approximately the shocked area. In such conditions, only few fragments of the shocked specimens could be recovered.

In the experiments conducted at the CESTA, the B-C specimens were inserted between a covering Al foil pasted on a 30-μm-thick Au foil and a thick Au backing plate (see Table I). The impedance mismatch between Al and Au leads to a significant amplification of the shock transmitted across the interface, which compensates the lower laser energy available on this facility. Besides, the use of Au is expected to prevent possible chemical reactions that might have occurred between Al and the shock-loaded B-C mixtures. A typical VISAR record of free-surface velocity is shown in Fig. 7. Again, the good agreement with simulations where the presence of the thin B-C sample in the multilayered assembly is disregarded allows inferring the pressure history from the computations. In all tests, the covering foils were removed by the shot (e.g., Fig. 7), so that only small amounts of the shocked B-C mixture could be recovered and analyzed.

IV. CHARACTERIZATION OF THE POSTSHOCKED B-C SAMPLES

Typical x-ray diffraction pattern of B-C sample recovered after shock compression is presented in Fig. 8. It shows a phase segregation of the original graphitelike B-C structure into a mixture of disordered (turbostratic) graphite and boron carbide, B_4C or $B_{13}C_2$. Similar products have been detected

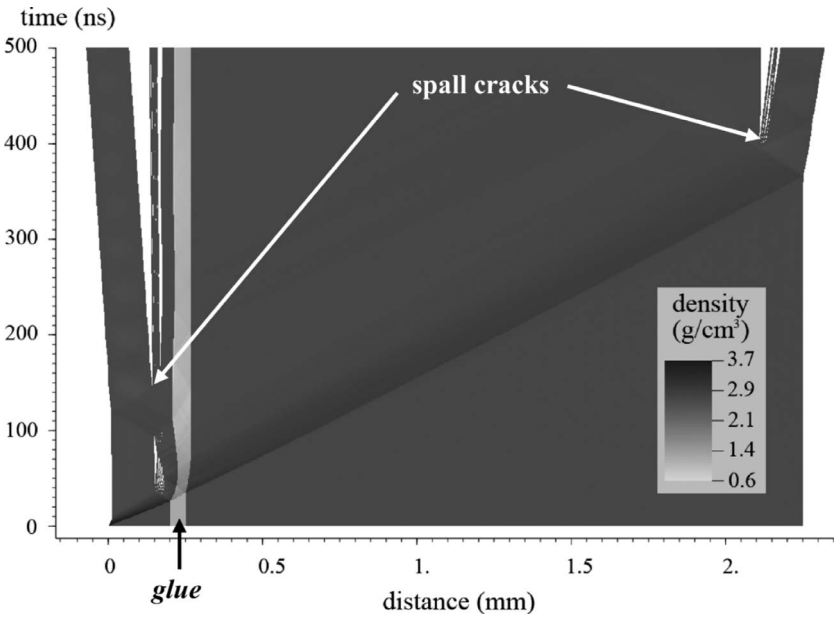

FIG. 5. Computed time-distance diagram showing the one-dimensional response of a three-layered target to a laser shock of 48 GPa. The geometry (50-μm-thick epoxy layer inserted between two Al plates) and the loading conditions are representative of shot BC_3 No. 1, disregarding the thin chip embedded inside the glue. The laser shock is applied at time 0 onto the left surface. The density contours clearly show the compression and release waves propagating in the target assembly, including the wave reverberation throughout the glue layer. The damage predicted by this simulation is consistent with the postshock observations in the recovered target (Fig. 4). It consists of the ejection of a first spalled layer from the covering Al plate (after about 150 ns and about 100–150 μm deep in this plate), followed by that of a second spall from the rear surface of the backing plate (after about 400 ns and about 100–150 μm deep beneath that surface).

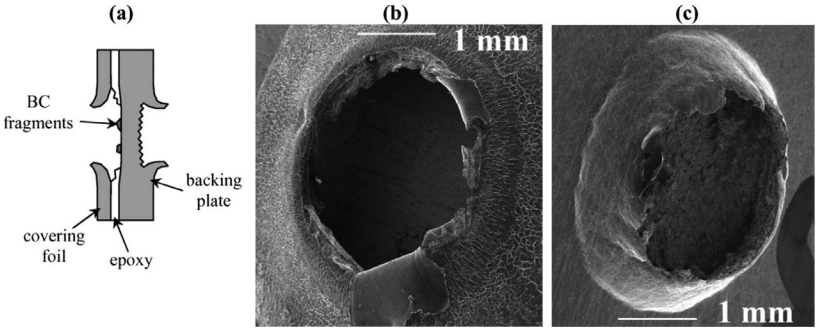

FIG. 6. (a) Schematic cross section of the target recovered after a 60 GPa laser shock (shot BC_3 No. 2) applied onto the left surface and scanning electron micrographs of the (b) covering Al foil and (c) backing Al plate. The right picture shows the spall crater resulting from the reflection of the transmitted pressure pulse from the back free surface.

in all recovered samples irrespective to their stoichiometry. No phase with diamondlike structure has been observed. Using the Scherrer formalism and experimental data on the linewidths of BC No. 2 sample, we have evaluated the length of coherent scattering for boron carbide as ~100 Å, and for turbostratic graphitelike phase as ~70 Å (~60 Å for starting *t*-BC phase) along the *c* direction and ~60 Å along the *a* direction (~20 Å for starting *t*-BC phase). Evidently, the coherent scattering domains of forming boron-doped graphite are larger because the starting-phase lattice with random distribution of B and C atoms passes into lattice with uniform distribution of C atoms of resulting graphitelike phase with much lower boron content. As expected, the effect is more remarkable for the *a* axis.

Raman spectroscopy is a versatile method for the characterization of carbon compounds. Advantage stands in the possibility of analyzing microscopic samples without any special preparation since very small samples' amounts were available after laser shock experiments. Actually Raman spectroscopy is highly sensitive to hybridization states of carbon between the sp^2 bonds of graphite (1583 cm^{-1}) and the sp^3 bonds of hexagonal diamond (1320 cm^{-1}). Moreover the main feature of the crystallographic description of carbon compounds is the comparison between the *D* band at ~1340 cm^{-1} characterizing the disorder of the crystalline lattice (Ref. 21 and related references) and the *G* band at ~1590 cm^{-1} characterizing the stretching mode of the C-C bonds (symmetry E_{2g}) in pure graphite layers. Figure 9 shows Raman spectra of microcrystalline and turbostratic graphite. The B-C samples recovered after shock loading were micrograins without any orientation. After Refs. 22 and 23 the intensity of the *G* band is independent of the polarization and then independent of the position of the microsamples. The intensity and shape of the *D* band depend only on the size of the grains, the nature of tracks, and/or the doping impurities such as boron[24,25] inserted into the graphite lattice. On the other hand, it is known[26] that the Raman cross section for graphite (sp^2) is ~50 times higher than for diamondlike bonds (sp^3) which means that, except for high concentrations of sp^3 bonds like in diamond, sp^3 hybridization would be difficult to detect.

Figure 10 shows spectra of two shock-compressed BC_3 samples in comparison with starting BC_3 and turbostratic graphite. Two main features are observed. Both starting material and final product are turbostratic. However, the increase in the ratio of $I(D)/I(G)$ intensities from 1.3 to 1.5 after shock compression indicates a higher disorder of the final product.[22,27,28] A second feature is the downshift of the frequencies of both *D* and *G* bands to 1340 and 1568 cm^{-1}, respectively.

Figure 11 shows Raman spectra of two shock-compressed B_2C_3 fragments recovered after shot B_2C_3 No. 2 in comparison with starting B_2C_3 and turbostratic graphite. The $I(D)/I(G)$ ratio of the starting B_2C_3 is 2.0 which is higher than that of turbostratic graphite (1.5) due to higher structural disorder of the B_2C_3 structure. The shock-compression behavior of B_2C_3 is different from that of BC_3. Actually, two different phases [spectra (3) and (4) in Fig. 11] have been recovered in the shock-loaded cell and characterized. Spectrum (3) is close to that of BC_3 up shifted by 5 cm^{-1}. The $I(D)/I(G)$ ratio of 2.2 is a little higher than for the starting B_2C_3, indicating an additional disturbance resulting from the shock. Spectrum (4) is similar to the Raman spectrum of strongly disordered $B_{4.3}C$ sample after indentation.[29] The

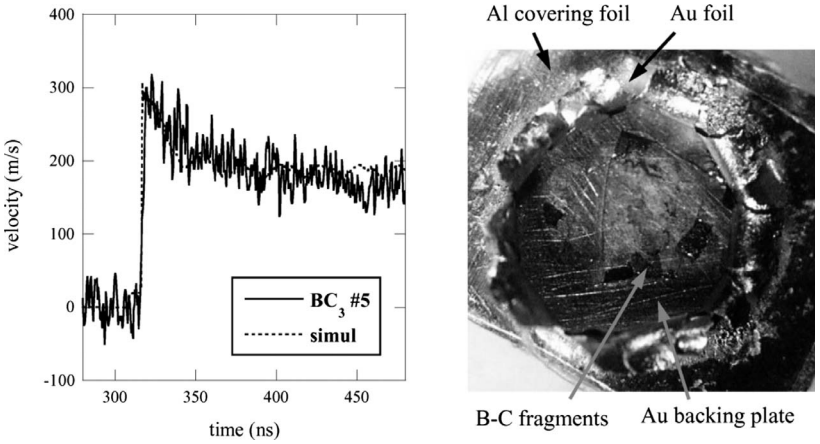

FIG. 7. Free-surface velocity profiles measured (solid line) and computed (dotted line) at the back of a multilayered target composed of an Al covering layer, a thin Au foil, a BC_3 specimen embedded in epoxy glue, and a thick Au backing plate (shot BC_3 No. 5; see Table I). An optical micrograph of the recovered target is shown on the right. The front foils have been torn outward by reflected waves, so that only few fragments of the BC_3 sample could be recovered.

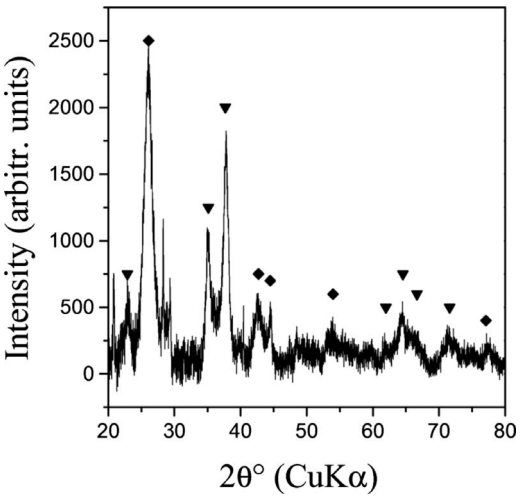

FIG. 8. X-ray diffraction pattern of the material recovered after shot BC No. 2. Diamonds and triangles show the reflections of disordered graphite and boron carbide, respectively.

weak feature at ~1460 cm^{-1} was not assigned.

V. DISCUSSION

Laser shock experiments were performed on B-C phases of different stoichiometry. Estimates of the loading pressure pulse were provided for each shot by hydrodynamic simulations of laser-matter interaction and wave propagation, which were found to be in good agreement with results of time-resolved velocity measurements, on one hand, and postshock observations, on the other hand. Despite the high amplitudes of the incident laser shocks, up to more than 70 GPa, the pressure and temperature transmitted into the B-C specimens probably outlaid the *p-T* conditions required for the phase transition into diamondlike structures. This is due to both the fast decay of the short pulse during its propagation through the covering foil and to the impedance mismatch between

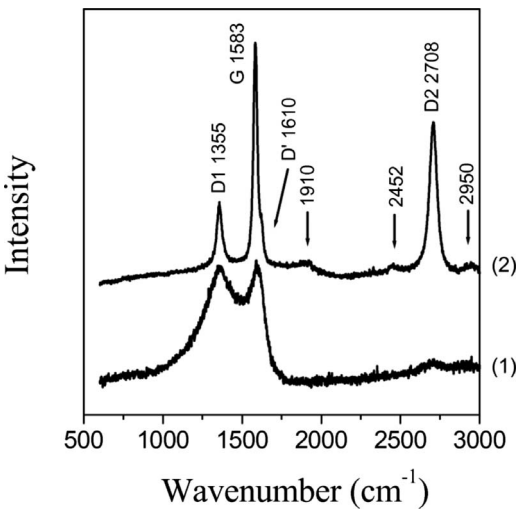

FIG. 9. Raman spectra of (1) turbostratic and (2) microcrystalline graphite.

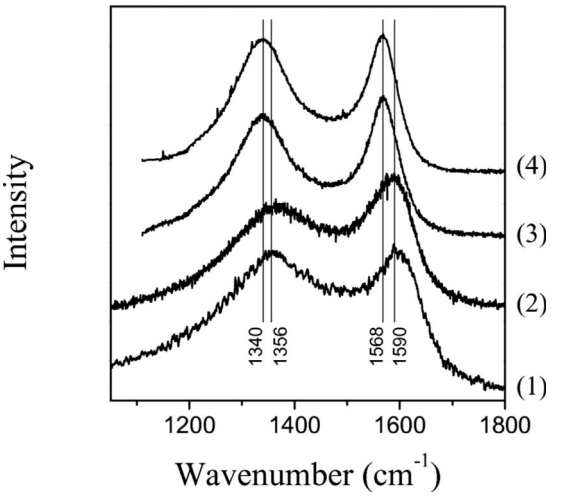

FIG. 10. Raman spectra of (1) and (2) laser-shocked BC_3 samples, (3) starting BC_3, and (4) turbostratic graphite.

this metallic foil and the glue surrounding the sample. An estimate of the shock-induced temperature in the immediate vicinity of the specimen was inferred from the loading pressure and shock wave data from the literature. Even for shocks of highest amplitudes, estimated temperature remains slightly below the 2300-K value required at quasihydrostatic conditions. Thus, the absence of diamondlike phase(s) in the recovered samples is probably due to insufficient loading pressure and/or temperature range. Furthermore, the very short time of pressure application (some ns) typical of laser-driven shocks can lead to some kinetic inhibition of structural transitions. Hence, the synthesis of such diamondlike structures under dynamic compression requires further work, including use of preheated targets, as well as explosive and impact techniques, for those the duration of the pressure load is in the range of few μs.

ACKNOWLEDGMENTS

We thank all the staff of the LULI and the Alisé team for

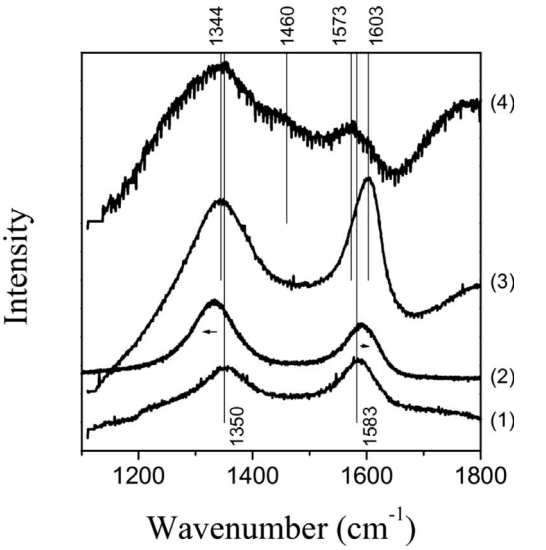

FIG. 11. Raman spectra of (1) turbostratic graphite, (2) starting B_2C_3, and (3) and (4) laser-shocked B_2C_3 fragments.

technical support, as well as Mustapha Jouiad from Laboratoire de Mécanique et Physique des Matériaux for his kind help with the SEM. The access to the LULI facility was provided by ILP (Institut Laser Plasma, FR 2707). This work was financially supported by the Agence Nationale de la Recherche (Grant No. ANR-05-BLAN-0141).

*resseguier@lcd.ensma.fr

[1] *The Nature of Diamonds*, edited by G. E. Harlow (Cambridge University Press, New York, 1998).
[2] J. Isberg, Science **297**, 1670 (2002).
[3] V. L. Solozhenko, N. A. Dubrovinskaia, and L. S. Dubrovinsky, Appl. Phys. Lett. **85**, 1508 (2004).
[4] V. L. Solozhenko, O. O. Kurakevych, D. Andrault, Y. Le Godec, and M. Mezouar, Phys. Rev. Lett. **102**, 015506 (2009).
[5] K. Kondo, S. Sogo, A. Sawaoka, and M. Araki, J. Mater. Sci. **21**, 1579 (1986).
[6] D. J. Erskine and W. J. Nellis, Nature (London) **349**, 317 (1991).
[7] C. S. Yoo, W. J. Nellis, M. L. Sattler, and R. G. Musket, Appl. Phys. Lett. **61**, 273 (1992).
[8] H. Hirai, K. Kondo, N. Yoshizawa, and M. Shiraishi, Appl. Phys. Lett. **64**, 1797 (1994).
[9] J. Hu, X. Zhou, H. Tan, J. Li, and C. Dai, Appl. Phys. Lett. **92**, 111905 (2008).
[10] T. de Rességuier, P. Berterretche, M. Hallouin, and J. P. Petitet, J. Appl. Phys. **94**, 2123 (2003).
[11] P. Berterretche, T. de Rességuier, M. Hallouin, and J. P. Petitet, J. Appl. Phys. **96**, 4233 (2004).
[12] T. Sano, H. Mori, E. Ohmura, and I. Miyamoto, Appl. Phys. Lett. **83**, 3498 (2003).
[13] T. Shirasaki, A. Derré, M. Ménétrier, A. Tressaud, and S. Flandrois, Carbon **38**, 1461 (2000).
[14] L. M. Barker and R. E. Hollenbach, J. Appl. Phys. **41**, 4208 (1970).
[15] W. F. Hemsing, Rev. Sci. Instrum. **50**, 73 (1979).
[16] T. Antoun, L. Seaman, D. R. Curran, G. I. Kanel, S. V. Razorenov, and A. V. Utkin, *Spall Fracture* (Springer, New York, 2002).
[17] G. I. Kanel and V. E. Fortov, Adv. Mech. **10**, 3 (1987).
[18] T. de Rességuier, S. Couturier, J. David, and G. Niérat, J. Appl. Phys. **82**, 2617 (1997).
[19] L. Tollier, R. Fabbro, and E. Bartnicki, J. Appl. Phys. **83**, 1231 (1998).
[20] *High-Velocity Impact Phenomena*, edited by R. Kinslow (Academic, New York, 1970), p. 557.
[21] E. Boccaleri, A. Arrais, A. Frache, W. Gianelli, P. Fino, and G. Camino, Mater. Sci. Eng., B **131**, 72 (2006).
[22] S. Reich and C. Thomsen, Philos. Trans. R. Soc. London, Ser. A **362**, 2271 (2004).
[23] M. Cardona, in *Light Scattering in Solids II*, Topics in Applied Physics, edited by M. Cardona and G. Güntherodt (Springer, New York, 1982), Vol. 50, p. 19.
[24] Y. Wang, D. C. Alsmeyer and R. McCreery, Chem. Mater. **2**, 557 (1990).
[25] C. Thomsen and S. Reich, Phys. Rev. Lett. **85**, 5214 (2000).
[26] A. C. Ferrari, Solid State Commun. **143**, 47 (2007).
[27] F. Tuinstra and J. L. Koenig, J. Chem. Phys. **53**, 1126 (1970).
[28] R. Moradian, J. F. Annett, B. L. Gyorffy, and G. Litak, Phys. Rev. B **63**, 024501 (2000).
[29] V. Domnich, Y. Gogotsi, M. Trenory, and T. Tanaka, Appl. Phys. Lett. **81**, 3783 (2002).